Carbohydrate Polymers 120 (2015) 74–84

Contents lists available at ScienceDirect

Carbohydrate Polymers

journal homepage: www.elsevier.com/locate/carbpol

Alginate–sterculia gum gel-coated oil-entrapped alginate beads for gastroretentive risperidone delivery

Hriday Bera [a,*], Saisharan Goud Kandukuri [a], Amit Kumar Nayak [b,*], Shashank Boddupalli [a]

[a] Department of Industrial Pharmacy, Gokaraju Rangaraju College of Pharmacy, Bachupally, Hyderabad 500090, India
[b] Department of Pharmaceutics, Seemanta Institute of Pharmaceutical Sciences, Mayurbhanj, Jharpokharia 757086, Odisha, India

ARTICLE INFO

Article history:
Received 8 November 2014
Received in revised form 6 December 2014
Accepted 12 December 2014
Available online 19 December 2014

Keywords:
Alginate
Sterculia gum
Olive oil
Floatation
Mucoadhesion
Risperidone

ABSTRACT

Novel floating-mucoadhesive oil-entrapped alginate beads coated with crossslinked alginate–sterculia gum gel membrane was developed for gastroretentive risperidone delivery. Oil-entrapped alginate beads containing risperidone as core were prepared by ionotropic gelation technique. Effects of polymer to drug ratio and oil to water ratio on drug entrapment efficiency (%) and cumulative drug release after 8 h (%) were studied to optimize the core beads by a 3^2 factorial design. The optimized beads (F—O) demonstrated drug entrapment efficiency of 83.73 ± 0.81% and cumulative drug release of 70.84 ± 0.27% after 8 h. The biopolymeric-coated optimized beads exhibited excellent buoyancy, better *ex vivo* mucoadhesion and slower drug release rate. The drug release profiles of risperidone-loaded uncoated and coated beads were best fitted in Korsmeyer–Peppas model with Fickian diffusion mechanism. The beads were also examined for the drug-excipients compatibility, drug crystallinity and surface morphology by FTIR, P-XRD and SEM analyses, respectively.

1. Introduction

Risperidone is an atypical anti-psychotic drug of benzisoxazole class, which is clinically recommended for bipolar disorder and schizophrenia management (Muthu & Singh, 2009). The variable half-life of it (3–20 h) has raised the interest in developing extended-release formulations of risperidone (Badshah et al., 2011). It exhibits an increased solubility at acidic pH relative to the solubility at alkaline pH (Prieto, Temprana, del Rio Zabala, Marotta, & Alonso Sdel, 2011). Therefore, a better drug dissolution and improved oral bioavailability can be ensured through prolonging the gastric residence of risperidone. Numerous oral sustained release gastroretentive drug delivery systems *viz.*, floating systems (Nayak, Pal, & Malakar, 2013; Malakar, Dutta, Purokayastha, Dey, & Nayak, 2014), mucoadhesive systems (Pal & Nayak, 2012), expandable or swellable systems (Klausner, Lavy, Friedman, & Hoffman, 2003), high density systems (Rouge et al., 1998), *etc.* have been developed. Recently, the combined floatation–mucoadhesion approaches for gastroretentive drug delivery have gained importance as these systems display an improved gastroretention by virtue of their floatation and bio-adhesion properties (Rathi, Medhekar, Pawar, Yewale, & Gudsoorkar, 2012; Malakar & Nayak, 2013). Currently, various natural polysaccharides are used in the development of gastroretentive drug delivery systems (Malakar, Nayak, & Pal, 2012; Nayak et al., 2013; Guru, Nayak, & Sahu, 2013).

Sodium alginate, a biodegradable, biocompatible, anionic natural heteropolysaccharide, able to form hydrogel beads by Ca^{2+} *etc.*, due to intermolecular ionotropic interactions between carboxylic acid groups of alginate molecules and calcium ions (Goh, Heng, & Chan, 2012). Calcium alginate beads have been intensively exploited as drug carriers in gastroretentive floating systems (Bera et al., 2009; Malakar et al., 2012). Unfortunately, alginate floating beads are suffered from low drug entrapment, less floating duration, long floating lag time and burst drug release, which can be improved by the incorporation of additives like low-density oils, effervescent agents, *etc.* Currently, oil-entrapped alginate floating beads have been established as promising multiple-unit vehicles for gastroretentive drug delivery due to their simplicity in preparation along with easy surface modification (Bera et al., 2009; Malakar & Nayak, 2012). Additionally, low-density oils improve the buoyancy and impose a hydrophobic barrier towards drug escaping from the matrices, which results in higher drug entrapment with prolonged drug release behavior (Malakar & Nayak, 2012).

Recently, a flurry of scientific investigations has employed mucoadhesive biopolymeric coating on gastroretentive floatable

* Corresponding authors at: Gokaraju Rangaraju College of Pharmacy, Department of Industrial Pharmacy, Bachupally, Hyderabad 500090, Andhra Pradesh, India and Seemanta Institute of Pharmaceutical Sciences, Department of Pharmaceutics, Mayurbhanj, Jharpokharia 757086, Odisha, India.
Tel.: +91 8977726256/+91 9583131603.
E-mail addresses: hriday.bera1@gmail.com (H. Bera), amitkrnayak@yahoo.co.in (A.K. Nayak).

http://dx.doi.org/10.1016/j.carbpol.2014.12.009
0144-8617/

systems (Sahasathian, Praphairaksit, & Muanqsin, 2010; Fahmy, 2012). Moreover, the usage of natural polysaccharides blends is a current trend to improve desired functional properties like drug encapsulation, swelling, drug release and stability (Ahuja, Yadav, & Kumar, 2010). Sterculia gum is a water-soluble polysaccharide obtained from the stem exudates of *Sterculia urens* (Singh, Sharma, & Chauhan, 2010). It is composed of partially acetylated polysaccharides of the substituted rhamnogalacturonoglycan, with residues of D-glucuronic acid, D-galacturonic acid, D-galactose and L-rhamnose (Singh & Sharma, 2008; Singh & Sharma, 2011). It exhibits excellent swelling with high viscosity and acid stability (Singh & Sharma, 2008). Thus, in the past few decades, an increased emphasis has been given on the usage of sterculia gum as a carrier in drug delivery (Deshmukh, Jadhav, & Sakarkar, 2009; Singh et al., 2010). Currently, crosslinked alginate–sterculia gum blend matrices are being used for the preparation of various multiple-unit drug delivery systems (Singh et al., 2010; Guru et al., 2013; Kulkarni, Patel, Nanjappaiah, & Naikawadi, 2014) including mucoadhesive beads (Krishna, Murthy, & Himabindu, 2009; Latheeshjlal, Satyanand, & Vaidya, 2013). Therefore, a mucoadhesive biopolymeric coating of ionotropically crosslinked alginate–sterculia gum blend gel onto oil-entrapped alginate beads would impart gastroretention by a combined mechanism of floatation and mucoadhesion, which was not investigated earlier. In the current investigation, oil-entrapped alginate beads containing risperidone were prepared by ionotropic emulsion gelation method. The prepared beads were optimized by a 3^2 factorial design, where the effects of independent factors, *i.e.*, polymer to drug ratio and oil to water ratio on responses, *i.e.*, drug entrapment efficiency and cumulative drug release after 8 h were studied. Finally, the optimized beads were coated with an ionotropically crosslinked alginate–sterculia gum gel membrane and evaluated for their different physical properties, buoyancy, *ex vivo* mucoadhesion and drug release behavior. The uncoated and coated optimized beads were also tested for drug-excipients compatibility, surface morphology and drug crystallinity.

2. Materials and methods

2.1. Materials

Risperidone (Mylan Ltd., India), sodium alginate (S.D. Fine Chemicals Ltd., India), sterculia gum (Nutriroma, India), olive oil (relative density = 0.91 g/cm^3, Qualigens Fine Chemicals, India) and calcium chloride ($CaCl_2$, Merck Ltd., India) were used. All the chemicals and reagents were of analytical grade.

2.2. Preparation of oil-entrapped alginate beads containing risperidone

Olive oil-entrapped alginate beads containing risperidone were prepared by ionotropic emulsion gelation technique (Bera et al., 2009). Initially, pre-gelation aqueous solutions of sodium alginate were prepared. To these solutions, required amount of risperidone and olive oil were dispersed and mixtures were homogenized at 5000 rpm for 30 min to ensure emulsion stabilization. Resultant emulsions were extruded using 21G needles into 5% w/v gently agitated $CaCl_2$ solutions (100 ml) at room temperature. The gelled beads were allowed to stand in the solution for 20 min before being separated and washed with 3 × 100 ml distilled water. After drying at room temperature for 24 h, beads were stored in the desiccators until used.

2.3. Experimental design

A 3^2 factorial design was adopted to evaluate the influence of independent factors such as polymer to drug ratio by weight (X_1) and oil to water ratio by volume (X_2) on the responses like drug entrapment efficiency (%) and cumulative drug release after 8 h (%) in simulated gastric fluid (pH 1.2). Two factors were varied at three different levels (high, medium and low) and the experimental trial was carried out on all nine possible combinations keeping other factors fixed (Table 1).

2.4. Coating onto oil-entrapped alginate beads containing risperidone

Optimized oil-entrapped alginate beads containing risperidone were placed in a 1.0% (w/w) alginate–sterculia gum (1:1) aqueous dispersion and subsequently introduced into $CaCl_2$ solution (5% w/v) to form a polymeric coating on the core beads. The beads were left to harden in the $CaCl_2$ solution for 10 min, washed with distilled water, and dried overnight at room temperature.

Table 1
Experimental plan of 3^2 factorial design (coded values in bracket) with observed response values and various physical characteristics.

Code	Factors with normalized levels		Responses		Diameter (mm)[a]	Density (gm/cm^3)[a]	Floating lag-time (min)[a]
	Polymer to drug ratio (by weight) (X_1)	Oil to water ratio (by volume) (X_2)	Drug entrapment efficiency (%)[a]	Cumulative drug release after 8 h (%)[a]			
F-1	5:1 (+1)	0.3:1 (+1)	87.76 ± 0.52	68.67 ± 0.76	2.21 ± 0.10	0.74 ± 0.13	4.10 ± 0.25
F-2	5:1 (+1)	0.175:1 (0)	79.70 ± 0.43	78.73 ± 0.60	1.80 ± 0.04	0.86 ± 0.02	4.20 ± 0.31
F-3	5:1 (+1)	0.05:1 (−1)	73.44 ± 1.02	82.73 ± 0.85	1.23 ± 0.13	0.91 ± 0.13	5.90 ± 0.20
F-4	3.5:1 (0)	0.3:1 (+1)	81.38 ± 0.34	68.47 ± 0.73	1.97 ± 0.06	0.66 ± 0.02	4.00 ± 0.41
F-5	3.5:1 (0)	0.175:1 (0)	75.53 ± 0.68	74.71 ± 0.83	1.63 ± 0.12	0.72 ± 0.05	3.80 ± 0.82
F-6	3.5:1 (0)	0.05:1 (−1)	70.37 ± 1.04	82.16 ± 0.71	1.24 ± 0.10	0.76 ± 0.16	4.10 ± 0.40
F-7	2:1 (−1)	0.3:1 (+1)	72.67 ± 0.90	64.29 ± 1.16	1.82 ± 0.09	0.61 ± 0.18	3.50 ± 0.53
F-8	2:1 (−1)	0.175:1 (0)	68.19 ± 0.18	70.77 ± 0.84	1.54 ± 0.12	0.65 ± 0.09	3.20 ± 0.61
F-9	2:1 (−1)	0.05:1 (−1)	64.10 ± 0.42	79.60 ± 0.52	1.11 ± 0.13	0.67 ± 0.17	2.80 ± 0.21
			Experimental values				
F—O	4.45:1	0.284:1	83.73 ± 0.81	70.84 ±0.27	2.13 ± 0.05	0.80 ± 0.13	4.80 ± 0.12
			Predicted values				
			84.94	69.98			
% Error[#]		+1.43	+1.43	−1.23			
F—O (coated)	4.45:1	0.284:1	81.63 ± 1.54	65.47 ± 0.59	2.49 ± 0.12	0.66 ± 0.15	4.12 ± 0.25

[a] Mean ± S.D; $n = 3$.
[#] Error (%) = [(predicted value − actual value)/predicted value] × 100.

2.5. Determination of drug entrapment efficiency

An accurately weighed 100 mg of risperidone-loaded beads was crushed and dissolved in 500 ml of simulated gastric fluid (pH 1.2) by stirring for 24 h using magnetic stirrer. The resulting solutions were then filtered using Whatman® filter paper (No. 40). The suitably diluted filtrate was assayed using a UV–visible spectrophotometer (Shimadzu/UV-1700, Japan) at 272 nm. The drug entrapment efficiency was calculated using the formula:

$$\text{drug entrapment efficiency}(\%) = \frac{\text{actual drug content}}{\text{theoretical drug content}} \times 100$$

2.6. Evaluation of bead size and density

The average bead size was determined after measuring the diameters of twenty beads from each batch by digital slide callipers (CD-6 CS, Mitutoyo Corporation, Japan). The mean weights of the beads were also measured and subsequently the densities of the beads were calculated using the following relationships (Malakar et al., 2012):

$$\rho = \frac{M}{V} \quad \text{and} \quad V = \frac{4}{3\pi r^3},$$

where ρ, M, V and r represent the density (g/cm^3), weight (g), volume (cm^3) and radius (cm) of the beads, respectively.

2.7. Surface morphology analysis

Beads were analyzed by a scanning electron microscope (SEM) (JOEL, Japan) equipped with secondary electron detector. The samples were coated with gold and examined at an accelerating voltage of 20 kV.

2.8. Fourier transform-infrared (FTIR) spectroscopy

The drug-excipient compatibility was assessed by FTIR spectroscope (Perkin Elmer, USA). The samples were prepared by KBr pellet method and the spectral scanning was conducted in wavelength region between 400–4000 cm^{-1}.

2.9. Powder X-ray diffraction (P-XRD) analysis

The drug crystallinity was evaluated using a powder X-ray diffractometer (Bruker-AXS D8) with a Cu$K\alpha$ radiation detector operating at 40 kV voltages and 30 mA current. The samples were analysed over 2θ range of 10–80° with a scan speed of 5°/min.

2.10. In vitro drug release study

The *in vitro* dissolution study was performed using USP Type-II dissolution apparatus (Electrolab, India) in 900 ml of simulated gastric fluid (pH 1.2) which was kept in a thermostatically controlled water bath maintained at 37 ± 0.5 °C with a paddle rotational speed of 50 rpm. An equivalent weight of beads containing 25 mg risperidone was placed into the dissolution medium. At regular time intervals, 5 ml of aliquots were collected and equal volume of fresh medium was replaced to maintain the sink condition. Collected samples were analyzed by a UV–visible spectrophotometer (Shimadzu/UV-1700, Japan) at 272 nm.

2.11. In vitro buoyancy study

The *in vitro* buoyancy of the uncoated and coated optimized beads containing risperidone was investigated following reported procedures with some modifications (Jain, Awasthi, Jain, & Agarwal, 2005). Fifty beads were placed in the dissolution apparatus type-II (Electrolab, India) containing 900 ml of simulated gastric fluid (pH 1.2) maintained at 37 ± 0.5 °C. The rotation speed was set at 50 rpm. The time required for rising to the surface of dissolution medium and the total beads remaining buoyant in acidic medium were recorded to estimate the buoyant lag-time and % buoyancy, respectively.

2.12. Evaluation of swelling index

The swelling behavior of the uncoated and coated optimized beads containing risperidone was examined in terms of % weight gain in simulated gastric fluid (pH 1.2) at 37 ± 0.5 °C. The beads were periodically withdrawn from the test media and weighed after removing the excess amount of water at the surface by using a blotting paper. Swelling index (%) was then calculated as:

$$\text{swelling index} = \frac{W_t - W_0}{W_0} \times 100,$$

where W_t is the weight of beads at time t and W_0 represents the weight of the beads before immersion.

2.13. Ex vivo mucoadhesion testing

The mucoadhesivity of the uncoated and coated optimized beads containing risperidone were tested by *ex vivo* wash-off method (Pal & Nayak, 2012). About 50 beads were spread on the freshly excised pieces of goat stomach mucosa (2 cm × 2 cm) tied onto a glass slide using threads. The tissue specimen was given a regular up-and-down movement in 900 ml of simulated gastric fluid (pH 1.2) at 37 ± 0.5° C contained in a vessel of the disintegration test apparatus. At predetermined time intervals, the number of beads still adhering to the tissue was recorded.

2.14. Data treatment

2.14.1. Optimization

The values of drug entrapment efficiency and cumulative drug release after 8 h of various trial oil-entrapped alginate beads were fitted into the 3^2 factorial design. Quadratic models including interactive and polynomial terms were generated to examine each response. The equation can be expressed as (Malakar et al., 2012):

$$Y = b_0 + b_1X_1 + b_2X_2 + b_3X_1X_2 + b_4{X_1}^2 + b_5{X_2}^2,$$

where Y is the response, b_0 is the arithmetic mean of responses of all the nine runs; b_i is the estimated coefficients for the independent factor X_i. X_1 and X_2 represent the individual effects, X_1X_2 displays interaction effects and polynomial terms (${X_1}^2$ and ${X_2}^2$) suggest the nonlinearity of the model. One-way ANOVA analysis was employed to investigate the significance of the models as well as individual independent variables ($p < 0.05$).

2.14.2. Kinetics modeling of drug release

The *in vitro* release data were fitted into various release equations and kinetic models like zero-order ($Q = kt + Q_0$), first-order ($Q = Q_0e^{kt}$), Higuchi ($Q = kt^{1/2}$), Hixson–Crowell ($Q^{1/3} = kt + {Q_0}^{1/3}$) and Korsmeyer–Peppas ($Q = kt^n$) model (Malakar & Nayak, 2012). Q represents the amount of drug released at time t, Q_0 is the initial value of Q and k is the release rate constant. The diffusion exponent (n) as mentioned in the Korsmeyer–Peppas model is the indicative of the drug release mechanism. When n is ≤0.45, it is Fickian diffusion. The n value between 0.45 and 0.89 is defined as anomalous transport. When n is ≥0.89, it is called case-II transport (Singh, Maity, & Sa, 2014).

2.14.3. Diffusion coefficient of drug

The diffusion coefficients of risperidone from the beads (cm^2/s) were determined employing following equation (Singh et al., 2014):

$$Dc = \pi \left(\frac{r\theta}{6M_\alpha} \right)^2,$$

where r is the equivalent spherical radius of the beads, θ represents the slope of linear portion of M_t/M_α versus $t^{1/2}$ plot, M_t indicates the amount of drug released at time t and M_α denotes the total amount of drug loaded.

2.14.4. Water penetration velocity

The water penetration velocity into the matrices was estimated from the % swelling data using following equation (Singh et al., 2014):

$$V = \frac{1}{2\rho A} \times \frac{dw}{dt},$$

where V indicates penetration velocity, dw/dt represents the slope of % swelling versus time curve, ρ is the density of water at 310 K and A denotes surface area of a beads.

2.14.5. Statistical analysis

Statistical optimization was carried out using Design-Expert 8.0.6.1 software (Stat-Ease Inc., USA). All measured data are expressed as mean ± standard deviation (S.D.) and analyzed by MedCalc® software.

3. Results and discussion

3.1. Preparation of oil-entrapped alginate core beads containing risperidone

Alginate is an anionic naturally occurring polysaccharide and is composed of an alternating sequence of (1–4)-linked α-L-glucuronic and β-D-mannuronic acid residues (Nayak et al., 2013). The alginate gel beads which are accomplished through the sol–gel transformation of alginate in presence of divalent cations like Ca^{2+}, Zn^{2+}, display promising roles in drug delivery (Goh et al., 2012). In the present investigation, various oil-entrapped alginate beads were prepared by the ionotropic emulsion gelation method using $CaCl_2$ as crosslinker (Table 1). When risperidone-loaded emulsions containing sodium alginate and olive oil were introduced to $CaCl_2$ solutions, the ionotropic interactions between the negatively charged carboxylic groups of alginate molecules and the positively charged calcium ions resulted in the formation of crosslinked 'egg-box' networks and yielded the gelled spheres, instantaneously.

3.2. Optimization of oil-entrapped alginate beads containing risperidone

A total nine trial formulations were prepared by employing a 3^2 factorial design. Different experimental trial formulations and the observed responses are displayed in Table 1. The results of ANOVA analysis revealed a statistically significant association between independent and response variables ($p < 0.05$) (Table 2). The generated model equations after eliminating insignificant terms ($p > 0.05$) on the basis of ANOVA results were:

Drug entrapment efficiency (%) = $75.49 + 5.99\,X_1 + 5.66\,X_2 + 1.44\,X_1X_2 - 1.47\,X_1^2$ [$R^2 = 0.993$; $p < 0.0001$] and cumulative drug release after 8 h (%) = $74.97 + 2.58\,X_1 - 7.18\,X_2$ [$R^2 = 0.961$; $p < 0.0001$].

Software generated three-dimensional response surface and corresponding two-dimensional contour plots illustrated the effects of the independent factors on the investigated responses (Fig. 1). The response surface plots as a function of two independent factors at a time are useful to study their main and interaction effects, simultaneously (Guru et al., 2013). The response surface and the corresponding contour plots relating drug entrapment efficiency demonstrated that increasing the polymer to drug ratio and oil to water ratio led to an improvement in the drug entrapment efficiency (Fig. 1a and b, respectively). In contrast, the response surface and the corresponding contour plots relating cumulative drug release after 8 h indicated that the drug release rate increased with increasing polymer to drug ratio and decreased with increasing oil to water ratio (Fig. 1c and d, respectively). The contour plots relating drug entrapment efficiency varied in a nonlinear pattern, indicating a nonlinear relationship between factors and drug entrapment efficiency (Fig. 1b). The contour plots relating drug release after 8 h suggested a linear relationship between factors and drug release (Fig. 1d).

A numerical optimization technique based on the criterion of desirability was adopted to develop the optimized formulation. The primary goal of the optimization process was to find the values of the independent factors that maximize the drug entrapment efficiency and minimize the cumulative drug release after 8 h. The desirable ranges of responses were restricted to 80 ≤ drug

Table 2
A summary of ANOVA analysis for the response variables.

Source	Sum of squares	d.f.[a]	Mean square	*F* value	*p*-Value[b]
(a) For drug entrapment efficiency (%) (quadratic model)					
Model	421.5	5	84.30	302.09	<0.0001 (s)
X_1	215.28	1	215.28	771.45	<0.0001 (s)
X_2	192.21	1	192.21	688.12	<0.0001 (s)
X_1X_2	8.27	1	8.27	29.62	0.0016 (s)
X_1^2	5.73	1	5.73	20.62	0.0040 (s)
X_2^2	0.50	1	0.50	1.84	0.2285 (ns)
Residual	1.67	6	0.28		
Total	423	11			
(b) For cumulative drug release after 8 h (%) (linear model)					
Model	351.20	5	70.24	45.93	<0.0001 (s)
X_1	39.89	1	39.89	26.08	0.0003 (s)
X_2	309.03	1	309.03	202.08	<0.0001 (s)
X_1X_2	0.39	1	0.39	0.26	0.6313 (ns)
X_1^2	1.41	1	1.41	0.92	0.3746 (ns)
X_2^2	0.069	1	0.069	0.045	0.8384 (ns)
Residual	9.18	6	1.53		
Total	360.37	11			

[a] d.f., degrees of freedom.
[b] *p* Value > 0.05 was considered as statistically significant. s and ns indicate significant and not significant, respectively.

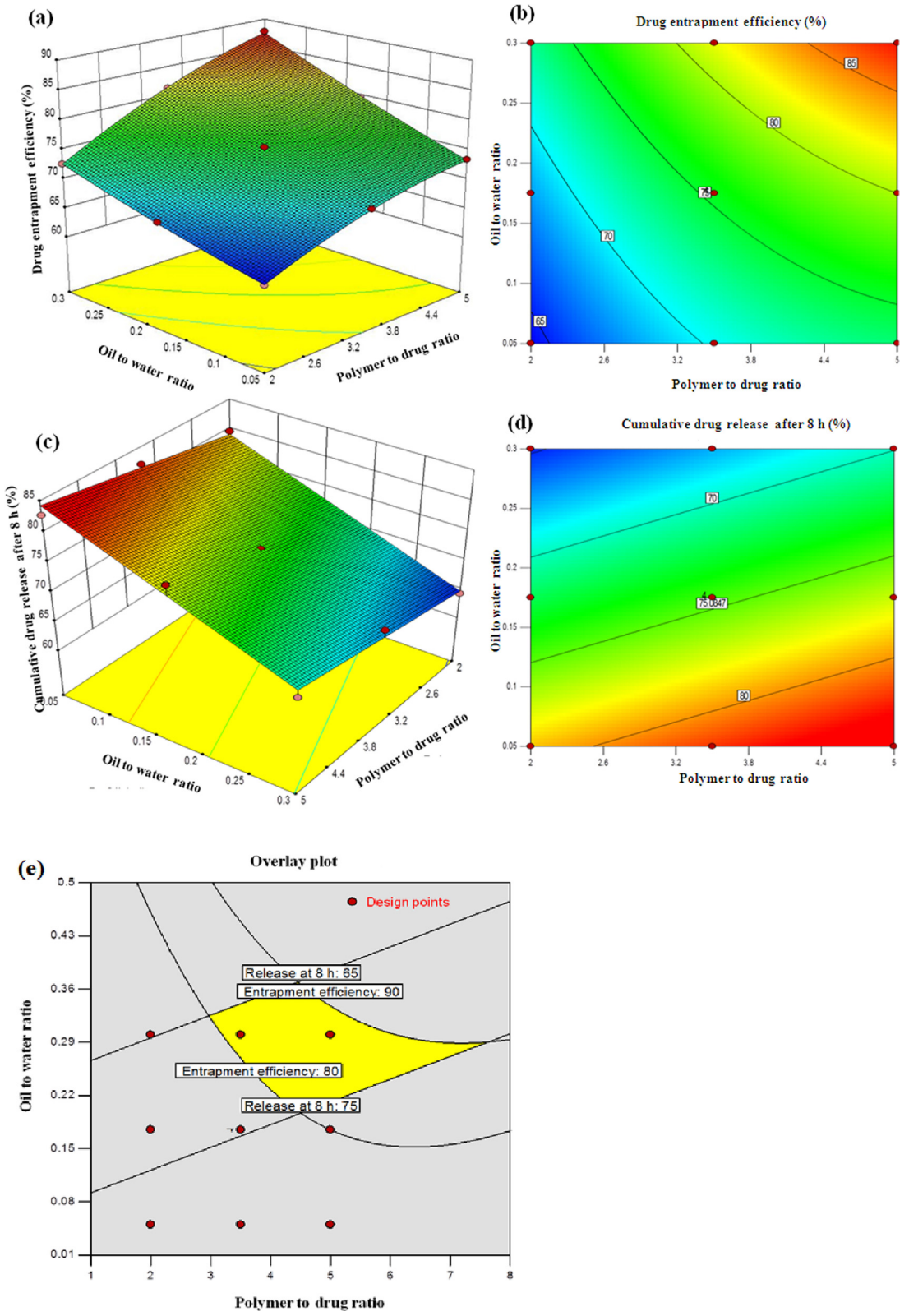

Fig. 1. Response surface 3D plots (a) and contour plots (b) demonstrating the effects of polymer to drug ratio by weight and oil to water ratio by volume on drug entrapment efficiency (%); response surface 3D plots (c) and contour plots (d) exhibiting the effects of polymer to drug ratio by weight and oil to water ratio by volume on cumulative drug release after 8 h (%); an overlay plot (e) illustrating the region of optimal process variable settings.

entrapment efficiency $\leq$ 90% and 65 $\leq$ cumulative drug release after 8 h $\leq$75%. The overlay plot as portrayed in Fig. 1e illustrated the region of optimal process variable settings. An optimal formulation setting having highest desirability near to 1.0 was selected among different settings recommended by Design Expert 8.0.6.1 software. The optimal values of polymer to drug ratio and oil to water ratio selected were 4.45% (w/w) and 0.284% (v/v), respectively. The confirmation experiments were conducted to test the

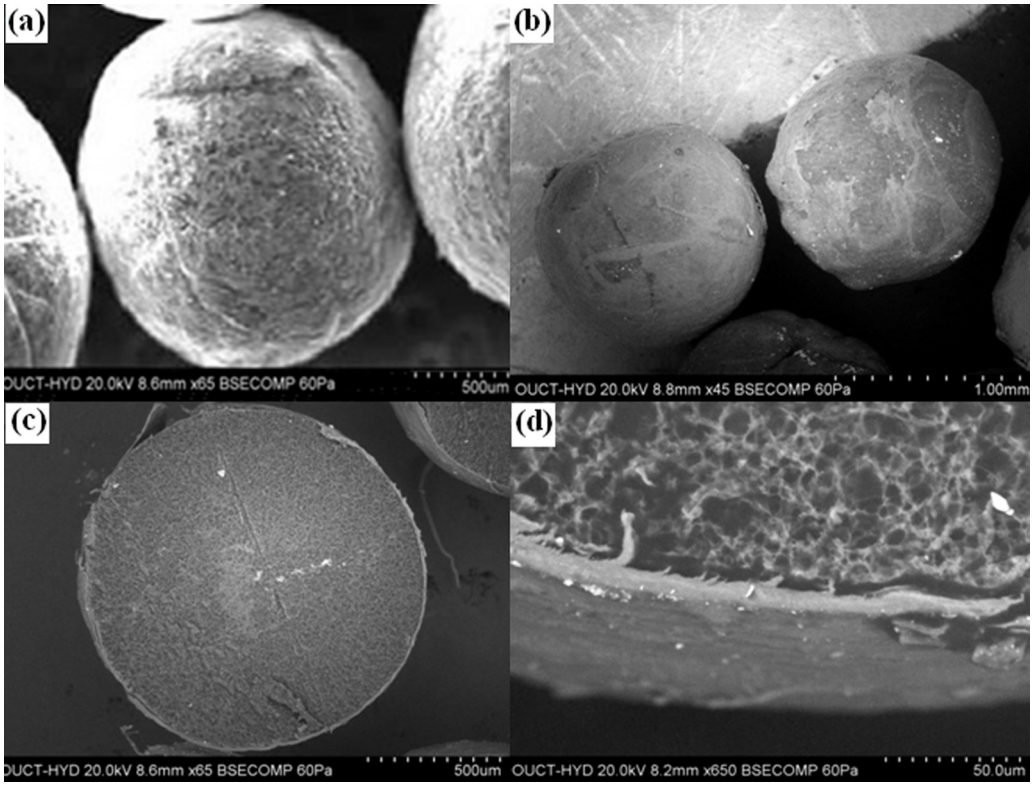

Fig. 2. Scanning electron microphotograph of the uncoated and coated oil-entrapped alginate beads (F—O) showing rough surface of the uncoated beads (a), smooth surface of the coated beads (b), cross-sectional view of the coated beads with less zoom (65×) (c) and high zoom (650×) (d).

responses of the optimal formulation (F—O). The experimental results and predicted responses are tabulated in Table 1. The relative errors between the predicted and observed values were +1.43 and −1.23% for drug entrapment efficiency and cumulative drug release after 8 h, respectively. In short, the experimental findings were within the close agreement to the model-based predictions, which conferred the predictability and validity of the models.

3.3. Coating on oil-entrapped alginate beads containing risperidone

The alginate matrix comprising an open lattice structure often produces porous beads and exhibits a lower retention capacity for low molecular weight drugs with high water solubility (Nayak & Pal, 2011). To overcome such inconveniences, alginate beads coated with natural polysaccharide polymers, alginate-natural polysaccharide blend beads, and interpenetrating or semi-interpenetrating polymer networks of alginate were developed (Sahasathian et al., 2010; Pal & Nayak, 2012; Kulkarni et al., 2014). In this study, the optimized formulation (F—O) was coated with an ionotropically crosslinked alginate–sterculia gum blend gel in order to achieve an enhanced gastric retention and sustained drug release rate. The optimized oil-entrapped alginate beads containing risperidone (F—O) were exposed to a dispersion of alginate–sterculia gum blend and subsequently introduced to the $CaCl_2$ solution. The ionotropic interactions between the negatively charged carboxylic groups of alginate and sterculia gum molecules and the positively charged calcium ions could lead to the formation of crosslinked biopolymeric membrane around the optimized beads. In addition, hydrogen bonding and electrostatic interactions between the two polysaccharides might be responsible for the membrane formation (Singh et al., 2010; Guru et al., 2013).

3.4. Drug entrapment efficiency

The drug entrapment efficiency of the oil-entrapped alginate beads containing risperidone varied from 64.10 ± 0.42 to 87.76 ± 0.52% (Table 1). The entrapment efficiency was highly influenced by the sodium alginate and olive oil contents. An increasing amount of alginate in the beads resulted in improved drug entrapment efficiency. In the presence of higher amount of polymer, a stronger interaction and/or entanglement of drug inside the ionotropically crosslinked alginate matrix was speculated (Malakar et al., 2012). Moreover, the drug entrapment efficiency increased with increasing oil inclusion, which might be due to higher partitioning of risperidone, a hydrophobic drug, in the oil phase. Oil might also form an insoluble barrier, which could obstruct the passage of drug molecules to the external media during preparation, leading to enhanced drug entrapment efficiency (Bera et al., 2009). The coated beads exhibited low drug entrapment efficiency relative to the uncoated optimized beads (F—O) (Table 1), which could possibly due to the leakage of small amount of drug during the coating process.

3.5. Bead size and density

The average size of the uncoated beads ranged from 1.11 ± 0.13 to 2.21 ± 0.10 mm (Table 1). The bead size appeared to increase with increasing polymer and oil concentrations. The incorporation of higher amounts of polymer and oil could lead to the formation of viscous emulsions and the beads formed from these emulsions became bigger in diameter (Malakar & Nayak, 2012). The alginate–sterculia gum gel-coated beads showed larger particle diameters than the uncoated beads (F—O). The density of risperidone-loaded uncoated beads was observed within the range, 0.61 ± 0.18–0.91 ± 0.13 g/cm^3 (Table 1). The decrease in density correlated with increased polymer and oil concentrations.

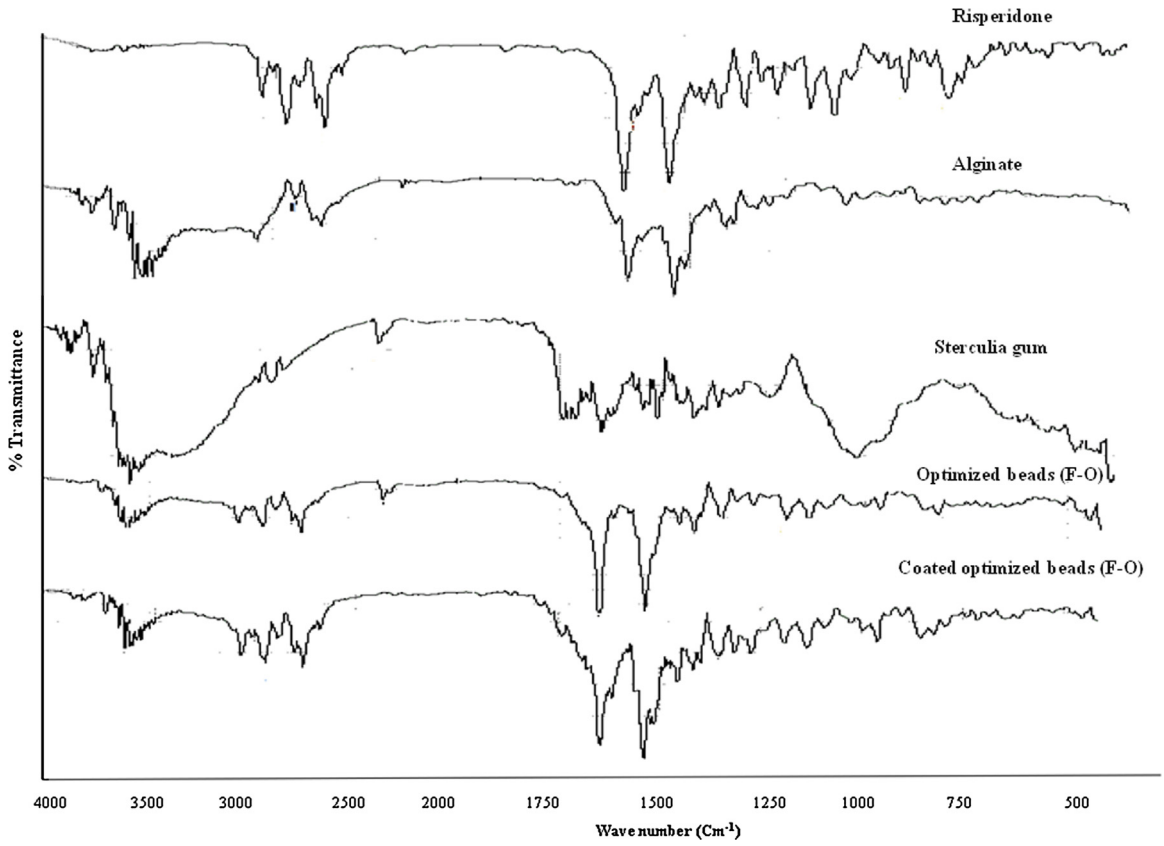

Fig. 3. The FTIR spectra of pure risperidone, alginate, sterculia gum, uncoated and coated optimized beads loaded with risperidone.

The density of the coated optimized beads was found to be lower relative to the uncoated optimized beads (F—O) due to the increased surface area after coating.

3.6. Surface morphology

The external surface and cross-sectional morphologies of the uncoated and coated optimized oil-entrapped alginate beads containing risperidone were examined by SEM analysis (Fig. 2). The SEM study of the uncoated beads exhibited a spherical shape with pores or wrinkles distributed throughout the surface, which could form as a result of the migration of water molecules during the drying process and subsequent shrinkage of the polymeric gel. The surface of the core beads was resembled to an orange-peel look (Fig. 2a). The absence of drug crystals on the surface of these beads indicated that the drug was in finely dispersed state in the alginate matrix (Malakar et al., 2012; Nayak et al., 2013). The SEM analysis of the coated beads revealed that they were almost spherical in shape and possessed smooth surface relative to the uncoated optimized beads as depicted in Fig. 2b. The coated membrane could reduce the number of cracks and pores on the outer surface of the beads. The cross-sectional view of the coated beads showed a sponge like structure, in which the oil was entrapped (Fig. 2c and d). The uneven size of the pores could be due to the coalescence of oil droplets during the gelation process. SEM micrograph of cross-sectional view of the coated beads showed that a thin-film membrane deposited onto the surface of the oil-entrapped beads as coating (Fig. 2c and d).

3.7. FTIR and P-XRD analyses

The FTIR spectra of risperidone, sodium alginate, sterculia gum, uncoated and coated optimized beads containing risperidone are presented in Fig. 3. In FTIR spectrum of risperidone, characteristic stretching and bending bands including N—O stretch, sharp, C=O stretch, sharp, CH_3 bending, CH_3 stretching, C—H asymmetric stretching of aromatic ring appeared around 1537, 1647, 1450, 2947, and 3068 cm^{-1}, respectively. The characteristic peaks of sodium alginate were evident at 3445, 1643, 1417 and 1130 cm^{-1}, which were due to the stretching of —OH, $—COO^-$ (asymmetric), $—COO^-$ (symmetric), and C—O—C, respectively. In the of FTIR spectrum of sterculia gum, absorption bands were observed at 3666, 1649 and between 1739 and 1240 cm^{-1} due to —OH, uronic acid and acetyl moieties, respectively. The FTIR spectra of the uncoated and coated optimized beads displayed all the characteristic peaks of sodium alginate, sterculia gum, and risperidone without any significant shifting. Thus, FTIR analysis confirmed that there was absence of any incompatibility of risperidone with the polymers used to develop uncoated and coated oil-entrapped floating beads.

The P-XRD patterns of pure risperidone, uncoated and coated optimized beads containing risperidone are shown in Fig. 4. P-XRD of risperidone exhibited the characteristic peaks at 11.3°, 14.2°, 18.6°, 19.3°, 21.2°, 23.0°, 28.8°, 44.0°, 64.4° and 77.5° (2θ) that were intense and sharp, indicating its crystalline nature. The diffraction pattern of risperidone in uncoated and coated optimized beads differed significantly to that of pure drug. It was observed that the sharp diffraction peaks corresponding to the drug almost disappeared in the P-XRD patterns of the formulations. The absence of the crystalline peaks of risperidone in P-XRD indicated that drug and excipients interacted strongly at molecular level, possibly drug formed a solid solution in oil blend matrix.

3.8. In vitro drug release

All the oil-entrapped alginate beads exhibited sustained risperidone release over 8 h in simulated gastric fluid (pH 1.2) (Fig. 5). The

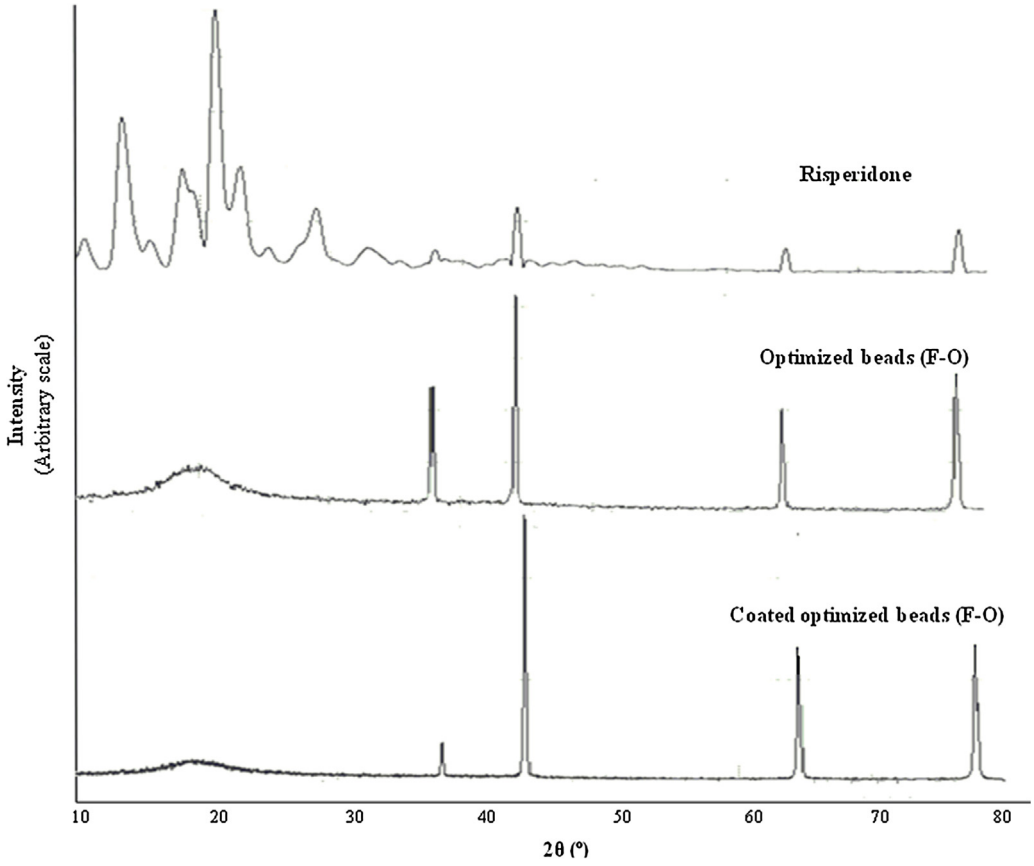

Fig. 4. The P-XRD patterns of pure risperidone, uncoated and coated optimized formulations containing risperidone.

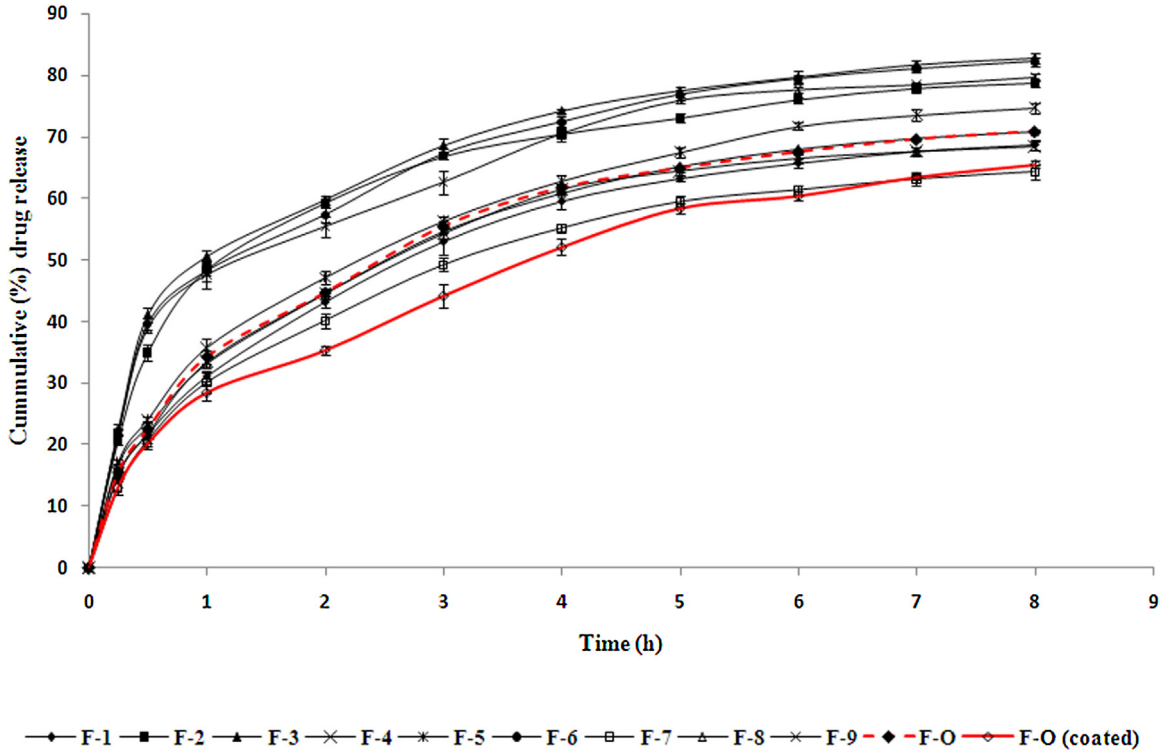

Fig. 5. The *in vitro* drug release profiles of the floating-mucoadhesive beads containing risperidone in simulated gastric fluid (pH 1.2). Results are presented as mean ± SD; SD denoted by error bars.

Table 3
Results of curve fitting of the *in vitro* drug-release profile of the mucoadhesive-floating beads in simulated gastric fluid (pH 1.2).

Code	Correlation coefficient (R^2)					Release exponent (n)
	Zero order	First order	Higuchi	Hixson–Crowell	Korsmeyer–Peppas	
F-1	0.842	0.926	0.974	0.522	0.987	0.45
F-2	0.735	0.883	0.918	0.427	0.939	0.35
F-3	0.737	0.907	0.919	0.419	0.933	0.34
F-4	0.820	0.904	0.964	0.509	0.979	0.44
F-5	0.847	0.947	0.977	0.513	0.989	0.43
F-6	0.760	0.919	0.932	0.431	0.946	0.34
F-7	0.842	0.918	0.974	0.522	0.981	0.46
F-8	0.841	0.931	0.975	0.512	0.989	0.43
F-9	0.761	0.909	0.931	0.430	0.946	0.34
F—O	0.832	0.924	0.970	0.513	0.982	0.44
F—O (coated)	0.891	0.958	0.990	0.550	0.993	0.45

cumulative drug released from different uncoated oil-entrapped beads after 8 h was found within the range of 68.67 ± 0.76 to 82.73 ± 0.85% (Table 1). Both independent factors showed significant influence on drug release. An increase in the concentration of alginate gave rise to higher drug release rate. However, a reverse phenomenon was observed in case of oil to water ratio. In acidic medium, the alginate matrix was converted to alginic acid, leading to a reduction in gel strength with an accelerated rate of drug release. The oil incorporation at higher level resulted in slower and sustained release of risperidone. The most reasonable explanation for the slow drug release was that the drug remained saturated and dispersed in the oil pockets of the beads to form a drug-oil dispersed matrix (Guru et al., 2013; Nayak et al., 2013). The drug transportation from the beads to the dissolution medium would follow a two-step process. The drug would initially diffuse from the oil pockets into the alginate matrix followed by transportation out of the polymeric matrix into the dissolution medium (Bera et al., 2009). The coated optimized beads exhibited a slower drug release profile than the uncoated beads (F—O). The coating membrane might be acted as a barrier to retard risperidone release from the oil-entrapped alginate beads. Moreover, the crosslinked alginate–sterculia gum gel coating could block the surface pores of the core beads (F—O), which would eventually lead to reduced water penetration and slower drug release rate.

The *in vitro* release data was fitted into zero-order, first-order, Higuchi, Hixson–Crowell and Korsemeyer–Peppas models to estimate the release kinetics. The results demonstrated that, in most cases, Korsmeyer–Peppas model was dominant with a correlation coefficient closer to 1 (Table 3). The calculated n values (Table 3) implied that the drug release of all the formulations was likely to be Fickian diffusion driven (Costa & Lobo, 2001). In the Fickian diffusion, the rate of water penetration into the polymeric matrices is slower than the rate of relaxation of the polymer chains. This behavior can be attributed to the rapid segmental mobility in the polymeric chains because of their low glass-transition temperature (T_g), which can minimize the polymer chain relaxation (Singh & Sharma, 2008).

3.9. Buoyancy

The buoyancy of the uncoated and coated oil-entrapped alginate beads containing risperidone is presented in Table 1 and Fig. 6a. The buoyancy correlated well with the mean density of these beads. It was evident that the density of all the formulations was less than that of simulated gastric fluid (*i.e.*, 1.004 g/cm^3) and thus, they exhibited floatation with a short floating lag time (less than 6 min) (Table 1). The incorporation of oil into the uncoated gel beads resulted in the formation of multiple tiny pockets within the polymer matrix, which played a pivotal role in buoyancy (Guru et al., 2013). The floating lag time decreased with increasing oil inclusion. The formulations containing a higher proportion of oil (F1, F3, F5 and F7) floated comparatively faster than those formulations (F2, F4, F6 and F8) with low oil contents. The buoyancy can also be attributed to the swelling and expansion of the matrix volume in aqueous media, leading to further decrease in beads density. The % buoyancy of the uncoated oil-entrapped beads depended on the polymer concentration. The % buoyancy decreased with increasing polymer concentration in the formulations. The coated beads displayed low lag time in floating with higher buoyancy (%) after 4 h and 8 h than the uncoated optimized beads (F—O) (Table 1 and Fig. 6a). The improved floating ability of the coated beads might be due to their low density and presence of an air compartment in between coating membrane and uncoated beads (Iannuccelli, Coppi, Bernabei, & Cameroni, 1998).

3.10. Swelling

The swelling of the uncoated and coated optimized oil-entrapped alginate beads containing risperidone was investigated in simulated gastric fluid (pH 1.2). The uncoated optimized beads (F—O) swelled up to 62.82 ± 3.29% at 8 h (Fig. 6b). The poor swelling of the uncoated optimized beads (F—O) may be attributed to the fact that the —COOH groups of the polymer, formed by de-crosslinking through the extraction of Ca^{2+} ions by Cl^- ions of the acid solution, remained unionized and did not induce the charge repulsion to increase the gel porosity and swelling of the matrices (Singh et al., 2014). The biopolymeric-coating onto optimized beads further reduced the swelling. Moreover, the slope of % swelling versus $\sqrt{}$ time plot (Table 4) conferred that the rate of swelling of the ionotropically crosslinked alginate–sterculia gum gel-coated beads in simulated gastric fluid was less than the uncoated optimized beads (F—O) (Fig. 6b). This was probably due to slow imbibitions of water molecules into the matrices. The water penetration velocity into the uncoated and coated matrices estimated from the % swelling (weight gain) data was found to be 0.0041 and 0.0067 cm/s, respectively. The values of the gel characteristic constant 'k' calculated from the intercepts of the $\ln M_t/M_\infty$ versus $\ln t$ plots were found to be different for uncoated and coated beads (Table 4) (Singh & Sharma, 2008), which could result in a variable penetration velocity of water molecules. The diffusion coefficients of the drug in the uncoated and coated beads were also determined based on Fickian diffusion model (Singh et al., 2014). The coated beads demonstrated a lower diffusion coefficient of the drug relative to the uncoated optimized beads (F—O) (Table 4). The biopolymeric-coating could restrict the polymer chains mobility upon contact with water and acted as a diffusion barrier for drug (Sahasathian et al., 2010).

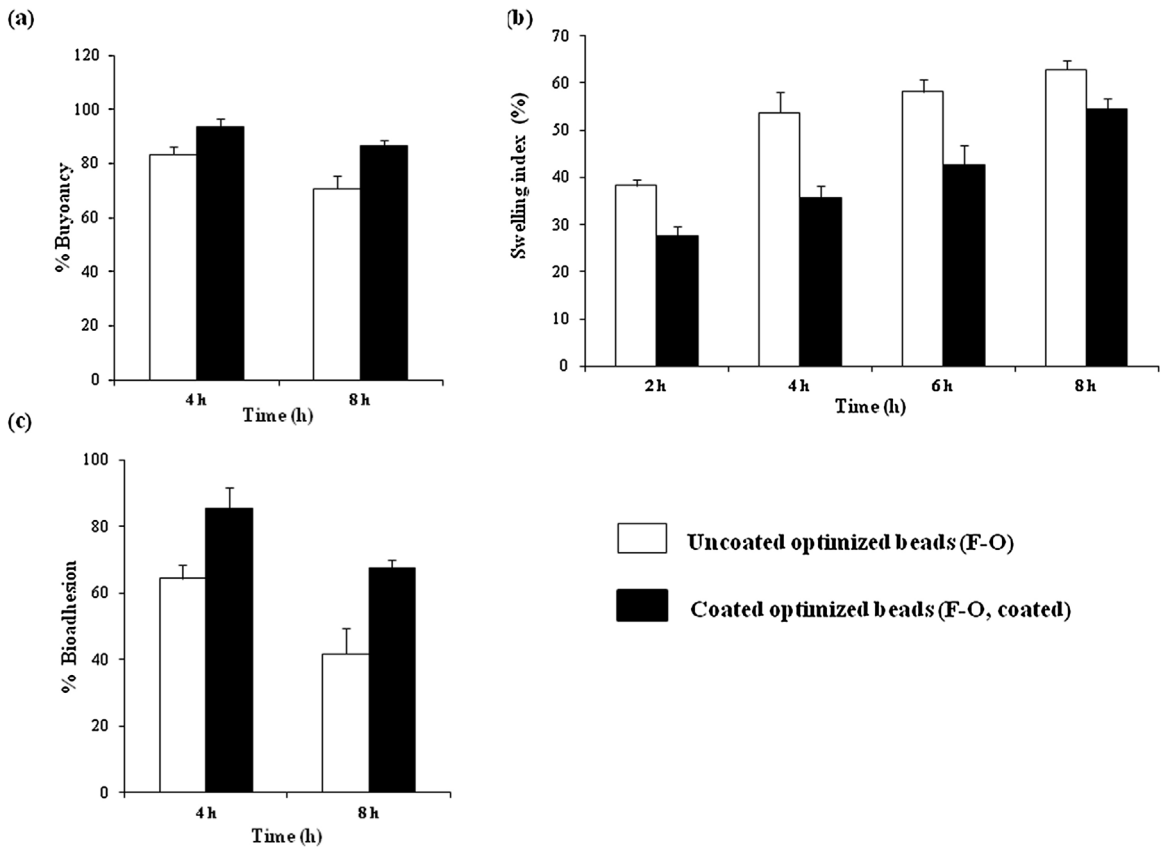

Fig. 6. The % buoyancy (a), swelling behavior (b) and mucoadhesivity (c) of the uncoated and coated optimized formulation (F—O) in simulated gastric fluid (pH 1.2). Results are presented as mean ± SD; SD denoted by error bars.

Table 4
Gel characteristic constant, swelling rate, water penetration velocity and diffusion coefficient of uncoated and coated optimized beads containing risperidone.

Code	Gel characteristic constant (k)	Swelling rate (%/$\sqrt{h}$)	Correlation coefficient (R^2)	Water penetration velocity (cm/s)	Diffusion coefficient (cm^2/s)
F—O	31.30	22.49	0.959	0.0067	2.15×10^{-8}
F—O (coated)	26.65	17.77	0.988	0.0041	2.09×10^{-8}

3.11. Mucoadhesivity

The results of *ex vivo* wash-off test performed using goat stomach mucosa in simulated gastric fluid (pH 1.2) are presented in Fig. 6c. It was observed that the *ex vivo* wash-off of oil-entrapped uncoated beads (F—O) was faster than the coated optimized beads. In simulated gastric fluid, the beads adhering to the mucosa were found to be 41.67 ± 7.64 and 67.67 ± 2.52% after 8 h for uncoated and coated optimized beads, respectively. The slow wash-off observed for coated beads could be due to the less ionization of functional groups in the polymeric coating that resulted in decreasing their solubility with enhanced adhesive strength (Sahasathian et al., 2010; Pal & Nayak, 2012). Therefore, the outcome of the wash-off test confirmed that the coated optimized beads had improved mucoadhesivity as compared to the uncoated optimized beads (F—O) containing risperidone.

4. Conclusion

The present work was dealt with the development and evaluation of floating-mucoadhesive alginate–sterculia gum gel-coated oil-entrapped alginate beads containing risperidone with an aim to prolong gastric residence time and enhance the bioavailability of the drug. The oil-entrapped alginate beads as core accomplished by ionotropic emulsion gelation method were optimized by employing a 3^2 factorial design. The optimized beads containing risperidone were further coated with ionotropically crosslinked alginate–sterculia gum gel membrane. The coated beads demonstrated improved buoyancy and mucoadhesivity with slower drug release profile. Overall, this study provided a simple, reproducible and economical approach for the development of biopolymeric-coated oil-entrapped alginate beads for intragastric delivery of risperidone.

Acknowledgments

The authors are thankful to Gokaraju Rangaraju Educational Society, Hyderabad, India and Seemanta Institute of Pharmaceutical Sciences, Mayurbhanj, India for providing essential laboratory facilities and support for this project. The authors also wish to express thanks to Mylan Ltd., India and Nutriroma, India for supplying Risperidone and sterculia gum, respectively as gift samples.

References

Ahuja, M., Yadav, M., & Kumar, S. (2010). Application of response surface methodology to formulation of ionotropically gelled gum cordial/gellan beads. *Carbohydrate Polymers*, *80*, 161–167.

Badshah, A., Subhan, F., Rauf, K., Bukhari, N. I., Shah, K., Khan, S., et al. (2011). Development of controlled-release matrix tablet of risperidone: influence of

Methocel(R)- and Ethocel(R)-based novel polymeric blend on *in vitro* drug release and bioavailability. *AAPS PharmSciTech*, *12*, 525–533.
Bera, R., Mondal, B., Bhowmik, M., Bera, H., Dey, S. K., Nandi, G., et al. (2009). Formulation and *in vitro* evaluation of sunflower oil entrapped within buoyant beads of furosemide. *Scientia Pharmaceutica*, *77*, 669–678.
Costa, P., & Lobo, J. M. S. (2001). Modeling and comparison of dissolution profiles. *European Journal of Pharmaceutical Sciences*, *13*, 123–133.
Deshmukh, V. N., Jadhav, J. K., & Sakarkar, D. M. (2009). Formulation and *in vitro* evaluation of theophylline anhydrous bioadhesive tablets. *Asian Journal of Pharmaceutics*, *3*, 54–58.
Fahmy, R. H. (2012). Statistical approach for assessing the influence of calcium silicate and HPMC on the formulation of novel alfuzocin hydrochloride mucoadhesive-floating beads as gastroretentive drug delivery system. *AAPS PharmSciTech*, *13*, 990–1004.
Goh, C. H., Heng, P. W. S., & Chan, L. W. (2012). Alginates as a useful natural polymer for microencapsulation and therapeutic applications. *Carbohydrate Polymers*, *88*, 1–12.
Guru, P. R., Nayak, A. K., & Sahu, R. K. (2013). Oil-entrapped sterculia gum-alginate buoyant systems of aceclofenac: Development and *in vitro* evaluation. *Colloids and Surfaces B: Biointerfaces*, *104*, 268–275.
Iannuccelli, V., Coppi, G., Bernabei, M. T., & Cameroni, R. (1998). Air compartment multiple-unit system for prolonged gastric residence. Part I. Formulation study. *International Journal of Pharmaceutics*, *174*, 47–54.
Jain, S. K., Awasthi, A. M., Jain, N. K., & Agarwal, G. P. (2005). Calcium silicate based microspheres of repaglinide for gastroretentive floating drug delivery: preparation and in vitro characterization. *Journal of Controlled Release*, *107*, 300–309.
Klausner, E. A., Lavy, E., Friedman, M., & Hoffman, A. (2003). Expandable gastroretentive dosage forms. *Journal of Controlled Release*, *90*, 143–162.
Krishna, R. R., Murthy, T. E. G. K., & Himabindu, V. (2009). Design and development of mucoadhesive microcapsules of glipizide formulated with gum karaya. *Journal of Pharmacy Research*, *2*, 208–214.
Kulkarni, R. V., Patel, F. S., Nanjappaiah, H. M., & Naikawadi, A. A. (2014). In vitro and *in vivo* evaluation of novel interpenetrated polymer network microparticles containing repaglinide. *International Journal of Biological Macromolecules*, *69*, 514–522.
Latheeshjlal, L., Satyanand, S., & Vaidya, M. (2013). Design and *in-vitro* comparative studies of glipizide microcapsules prepared by different polymers. *International Journal of Pharmacy and Pharmaceutical Sciences*, *5*, 267–269.
Malakar, J., Dutta, P., Purokayastha, S. D., Dey, S., & Nayak, A. K. (2014). Floating capsules containing alginate-based beads of salbutamol sulfate: *In vitro-in vivo* evaluations. *International Journal of Biological Macromolecules*, *64*, 181–189.
Malakar, J., & Nayak, A. K. (2012). Formulation and statistical optimization of multiple-unit ibuprofen-loaded buoyant system using 2^3-factorial design. *Chemical Engineering Research and Design*, *90*, 1834–1846.
Malakar, J., & Nayak, A. K. (2013). Floating bioadhesive matrix tablets of ondansetron HCl: Optimization of hydrophilic polymer-blends. *Asian Journal of Pharmaceutics*, *7*, 174–183.
Malakar, J., Nayak, A. K., & Pal, D. (2012). Development of cloxacillin loaded multiple-unit alginate-based floating system by emulsion–gelation method. *International Journal of Biological Macromolecules*, *50*, 138–147.
Muthu, M. S., & Singh, S. (2009). Poly (D, L-lactide) nanosuspensions of risperidone for parenteral delivery: Formulation and *in-vitro* evaluation. *Current Drug Delivery*, *6*, 62–68.
Nayak, A. K., & Pal, D. (2011). Development of pH-sensitive tamarind seed polysaccharide-alginate composite beads for controlled diclofenac sodium delivery using response surface methodology. *International Journal of Biological Macromolecules*, *49*, 784–793.
Nayak, A. K., Pal, D., & Malakar, J. (2013). Development, optimization and evaluation of emulsion-gelled floating beads using natural polysaccharide-blend for controlled drug release. *Polymer Engineering and Science*, *53*, 338–350.
Pal, D., & Nayak, A. K. (2012). Novel tamarind seed polysaccharide-alginate mucoadhesive microspheres for oral gliclazide delivery. *Drug Delivery*, *19*, 123–131.
Prieto, M. J., Temprana, C. F., del Rio Zabala, N. E., Marotta, C. H., & Alonso Sdel, V. (2011). Optimization and *in vitro* toxicity evaluation of G4 PAMAM dendrimer-risperidone complexes. *European Journal of Medicinal Chemistry*, *46*, 845–850.
Rathi, M., Medhekar, R., Pawar, A., Yewale, C., & Gudsoorkar, V. (2012). Floating and bioadhesive delivery system of metoprolol succinate: Formulation, development and *in vitro* evaluation. *Asian Journal of Pharmaceutics*, *6*, 227–236.
Rouge, N., Allemann, E., Gex-Fabry, M., Balant, L., Cole, E. T., Buri, P., et al. (1998). Comparative pharmacokinetic study of a floating multiple-unit capsule, a high density multiple-unit capsule and an immediate-release tablet containing 25 mg atenolol. *Pharmaceutical Acta Helbetiae*, *73*, 81–87.
Sahasathian, T., Praphairaksit, N., & Muanqsin, N. (2010). Mucoadhesive and floating chitosan-coated alginate beads for the controlled gastric release of amoxicillin. *Archives of Pharmacal Research*, *33*, 889–899.
Singh, B., & Sharma, N. (2008). Development of novel hydrogels by functionalization of sterculia gum for use in anti-ulcer drug delivery. *Carbohydrate Polymers*, *74*, 489–497.
Singh, B., & Sharma, N. (2011). Design of sterculia gum double potential antidiarrhoeal drug delivery system. *Colloids and Surfaces B: Biointerfaces*, *82*, 325–332.
Singh, B., Sharma, V., & Chauhan, D. (2010). Gastroretentive floating sterculia–alginate beads for use in antiulcer drug delivery. *Chemical Engineering Research and Design*, *88*, 997–1012.
Singh, P., Maity, S., & Sa, B. (2014). Effect of ionic crosslink on the release of metronidazole from partially carboxymethylated guar gum tablet. *Carbohydrate Polymers*, *106*, 414–421.